Available online at www.sciencedirect.com
SCIENCE DIRECT®
European Polymer Journal 40 (2004) 1743–1748
EUROPEAN POLYMER JOURNAL
www.elsevier.com/locate/europolj

Effects of organo-montmorillonite dispersion on thermal stability of epoxy resin nanocomposites

Baochun Guo *, Demin Jia, Changgeng Cai

Department of Polymer Materials and Engineering, South China University of Technology, Guangzhou 510640, China

Received 14 January 2004; received in revised form 25 March 2004; accepted 25 March 2004
Available online 8 May 2004

Abstract

Montmorillonite (MMT) was modified with the acidified cocamidopropyl betaine (CAB) and the resulting organo-montmorillonite (O-MMT) was dispersed in an epoxy/methyl tetrahydrophthalic anhydride system to form epoxy nanocomposites. The dispersion state of the MMT in the matrix was investigated by X-ray diffraction and scanning electronic microscopy. The thermal stability of the epoxy nanocomposites was examined by TGA. Thermal stability of the epoxy nanocomposite is dependent upon the dispersion state of the OMMT in the epoxy matrix although all the epoxy nanocomposites had enhanced thermal stability compared with the neat epoxy resin. The thermal stability of the epoxy resin nanocomposites was correlated with the dispersion state of the MMT in the epoxy resin matrix.

Keywords: Epoxy resin; Montmorillonite; Nanocomposite; Thermal stability; Structure

1. Introduction

Naturally occurred layered silicates like montmorillonite (MMT), hectorite, and saponite have received much attention as reinforcing materials for polymers because of their potentially high aspect ratio and unique intercalation/exfoliation characteristics [1,2]. Such clay minerals have a layered structure, typically about 1 nm in thickness and a high aspect ratio ranging from 100 to 1500, that with proper exfoliation can lead to platelets with high stiffness and strength dispersed in the polymer matrix [3–6].

Previous paper demonstrated a facile and effective process to prepare epoxy resin/montmorillonite nanocomposites by introducing catalytic centers into the galleries of MMT layers [7]. It has been proved that the properties especially mechanical properties of polymer/silicate nanocomposites are largely dependent of the degree of intercalation/exfoliation of the layered silicate in the polymer matrix. As the barrier properties of layered silicate to heat and oxygen, the dispersion state of the silicate or the degree of exfoliation of the silicate is especially crucial to the improvement of the thermal stability of the polymer/layered silicate nanocomposites. In the present paper, the thermal stability of the epoxy resin/MMT nanocomposites were studied and correlated with the dispersion state of the MMT in the epoxy resin matrix.

2. Experimental

2.1. Raw materials

Bisphenol A epoxy resin DER 331 with an epoxy value of 0.51 was obtained from Dow Chemical. The curing agent and accelerator were liquid methyl tetrahydrophthalic anhydride and 2-ethyl-4-methyl imidazole, respectively. Both of these were commercial

* Corresponding author. Tel.: +86-208-711-3374; fax: +86-203-867-2016.
E-mail address: psbcguo@scut.edu.cn (B. Guo).

0014-3057/$ - see front matter © 2004 Elsevier Ltd. All rights reserved.
doi:10.1016/j.eurpolymj.2004.03.027

products of chemical pure grade. Sodium MMT with ion-exchange capacity of 100 mequiv/100 g was purchased from Nanhai Nonmetals Minerals Co. (China). CAB with a solid content of 40% was supplied by Zhejiang Approval Technology Development Co., Ltd. (China).

2.2. Preparation of organo-montmorillonite (O-MMT) [7]

The sodium MMT was dispersed in distilled water, and the resulting solution was heated to about 80 °C. The acidified CAB with a determined amount was added dropwise to the solution under stirring. After the addition, the exchange lasted for about 8 h. The organoclay was filtered and washed thoroughly with distilled water and then dried in an oven thoroughly.

2.3. Preparation of epoxy resin nanocomposites [7]

The organoclay was mixed with epoxy resin at 80 °C for about 2 h. An almost transparent solution was obtained. When the resin was cooled to room temperature, methyl tetrahydrophthalic anhydride and 2-ethyl-4-methyl imidazole were added under stirring. The amounts of the anhydride and imidazole were 80 and 1 phr relative to the 100 phr resin. The well-mixed system was poured into a Teflon-coated mold, which was preheated to 60 °C and degassed for 1 h. The resin was then cured at 80 °C/1 h, 140 °C/1 h, and 150 °C/2 h. The cured resin was cooled naturally. All parts of the organoclay were relative to 100 phr of epoxy resin.

2.4. Characterizations

X-ray diffraction (XRD) measurements on the power samples and epoxy plates were performed with a D/MAX-III power diffractometer equipped with Cu K_α radiation ($\lambda = 1.54$ Å).

The morphology developed in the epoxy resin nanocomposite was examined with A Cambridge S 440 scanning electron microscope. The samples were fractured in liquid nitrogen and then coated with a thin gold–palladium before SEM.

Thermal gravimetric analysis (TGA) was carried out on a TA Instruments TGA 2050 under nitrogen purging at the heating rate of 10 °C/min from 30 to 600 °C.

3. Results and discussion

3.1. Dispersion of OMMT in the epoxy matrix

The XRD patterns of the epoxy resin nanocomposites with different OMMT content are shown in Fig. 1. When the OMMT loading is lower than 8 phr (relative to 100 phr resin), the d001 reflection is disappeared, indicating complete exfoliation of OMMT layers in the epoxy resin matrix. When the content of OMMT increases further, however, the weak d001 reflection is observed, indicating aggregation of OMMT in the epoxy resin matrix. These observations are accordant with the results of TEM [7], i.e. exfoliation/intercalation structure is developed in the composites with OMMT content higher than 8 phr. The dispersion of OMMT in the matrix was also examined with SEM, as shown in Fig. 2. It is shown that the OMMT is evenly dispersed in the matrix in the samples with lower OMMT content (4 and 6 phr). When the OMMT loading is higher than 8 phr, apparent aggregation of OMMT is observed although the aggregated OMMT remains an intercalated structure [7].

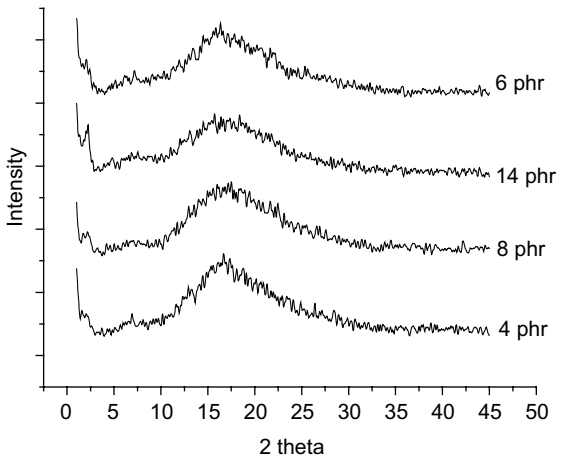

Fig. 1. XRD patterns of epoxy resin nanocomposites with different OMMT content.

3.2. Thermal stability

The effects of OMMT loading on the decomposition behavior are shown in Fig. 3. It is clearly shown that the nanoscale OMMT (platelets or tactoids) incorporated in the matrix improve the thermal stability of the epoxy resin. When the OMMT loading is lower than 8 phr, the samples exhibited higher thermal stability than those with higher OMMT loading. The characteristics of the thermal gravimetric curves are summarized in Table 1. The weight remaining at the characteristic temperature reaches a maximum at 6 phr OMMT loading.

To evaluate the thermal stability more detailed, nonisothermal thermal degradation kinetics were calculated. For an n-order reaction, the reaction rate can expressed as:

$$\frac{d\alpha}{dt} = k(1-\alpha)^n \quad (1)$$

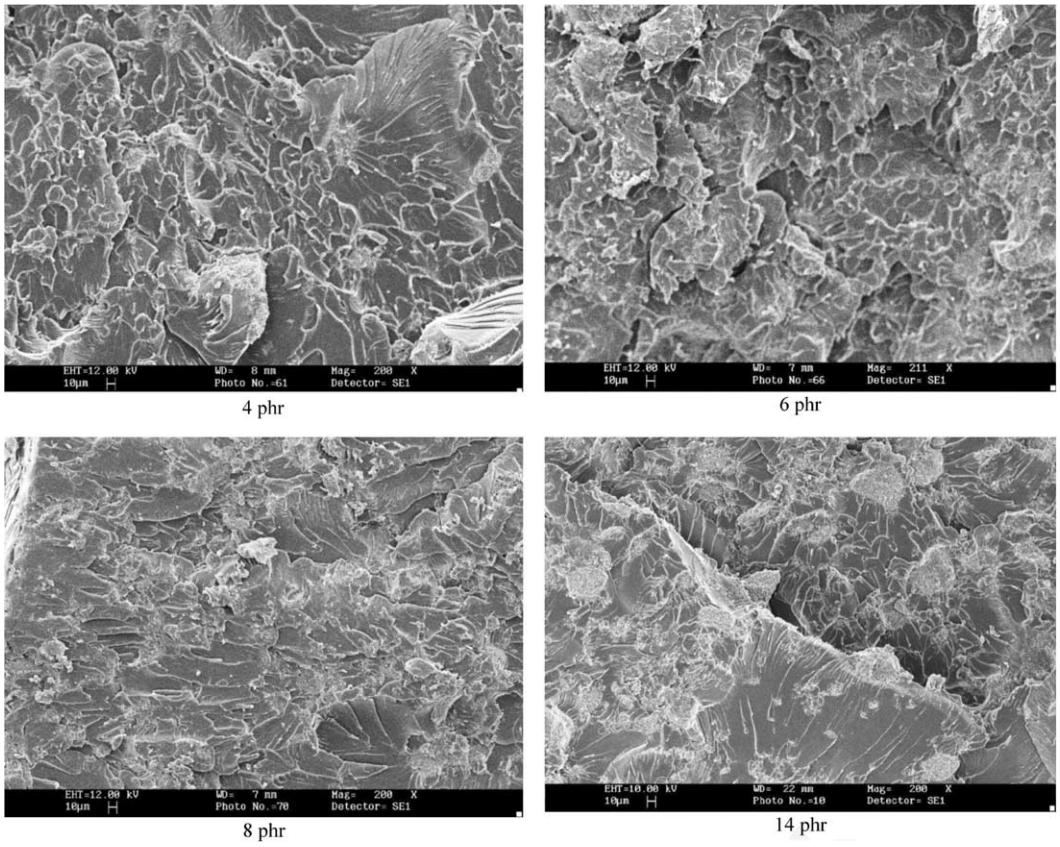

Fig. 2. SEM photos of epoxy nanocomposites with different OMMT loading.

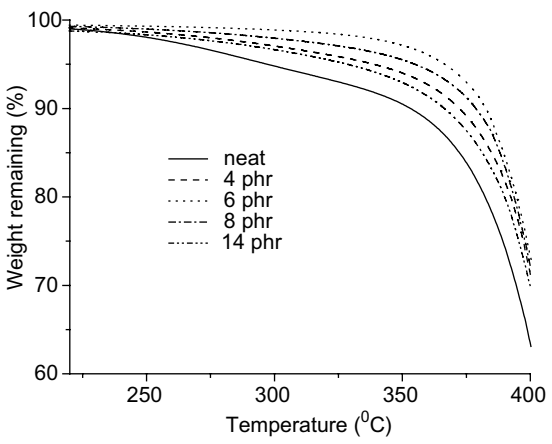

Fig. 3. Weight residue curves of epoxy nanocomposites.

where α is the apparent conversion, k is the rate constant, n is the reaction order.

In dynamic mode, the rate expression can be written as:

$$\frac{d\alpha}{dT} = \frac{A}{\phi}\exp\left(\frac{-E}{RT}\right)(1-\alpha)^n \tag{2}$$

where α is the conversion at temperature T, dependent on the heating rate ϕ, E is the apparent activation energy and A is the Arrhenius frequency factor.

Different kinetics expressions could be obtained by integrating the above equation with different approximation treatments. Among those kinetics equations, the Coats–Redfern equation [8] is one of the well-known models:

$$\ln\left[\frac{g(\alpha)}{T^2}\right] = \ln\left[\frac{\frac{AR}{\phi E}}{1-\frac{2RT}{E}}\right] - \frac{E}{RT} \tag{3}$$

where

$$g(\alpha) = \frac{1-(1-\alpha)^{1-n}}{1-\alpha}$$

If the order is equal to 1,

$$g(\alpha) = \ln(1-\alpha)$$

Table 1
TGA data of epoxy nanocomposites

Weight remaining (%)	0 phr	4 phr	6 phr	8 phr	14 phr
90	**353**	**372**	**383**	**379**	**366**
80	383	392	395	394	390
70	395	401	402	402	400
60	402	407	408	408	407
Char yield 580 °C (%)	6.46	9.18	8.80	10.34	12.83

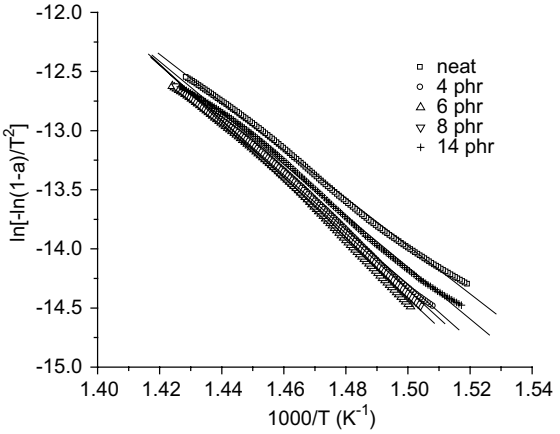

Fig. 4. Kinetics of thermal decomposition of epoxy nanocomposites by using Coats–Redfern equation.

$$\ln\left[\frac{\ln(1-\alpha)}{T^2}\right] = \ln\left[\frac{\frac{AR}{\phi E}}{1-\frac{2RT}{E}}\right] - \frac{E}{RT} \tag{4}$$

For the decomposition of thermosets, the mechanism of random scission of molecules dominates. Therefore the decomposition could be treated as one order reaction. The curves of $g(\alpha) = \ln(1-\alpha)$ versus $1000/T$ were computed with conversion. The activation energy could be calculated from the slope of the line. Fig. 4 shows the Coats–Redfern curve treated with one order reaction. The apparent activation energies are tabulated in Table 2.

Energy of activation for decomposition of epoxy nanocomposites can also be calculated from TGA curves by the integral method of Horowitz and Metzger [9] according to the following equation:

$$\ln\left[\ln\left(\frac{1}{1-\alpha}\right)\right] = \frac{E_a\theta}{RT_{max}^2} \tag{5}$$

where α is the decomposed fraction, E_a the activation energy for decomposition, T_{max} the temperature at maximum rate of weight loss, $\theta = T - T_{max}$, and R the gas constant.

From the plots of $\ln[\ln(\frac{1}{1-\alpha})]$ versus θ, which are shown in Fig. 5, the activation energy for decomposition can be calculated from the slope of the straight line in Eq. (5). The calculated activation energy as a function of the OMMT loading is shown in Fig. 6. As shown in Table 2 and Fig. 6, the activation energy is dependent on the OMMT loading. The activation energy of the nanocomposites reaches a maximum at 6 phr OMMT.

In addition, thermal stability has also been characterized by given integral procedural decomposition temperature (IPDT). Fig. 7 shows the schematic diagram of Doyle's proposition [10] for determining the IPDT of a major factor on thermal stabilities of the samples and the IPDT is calculated as follows:

$$\mathrm{IPDT} = \frac{(A_1+A_2)^3}{A_1(A_1+A_2+A_3)^2}(T_f - T_i) + T_i \tag{6}$$

Table 2
Kinetic data of epoxy nanocomposites by using Coats–Redfern equation

OMMT loading (phr)	E (kJ/mol)
0 (neat epoxy)	168.4
4	193
6	205.5
8	198.4
14	181

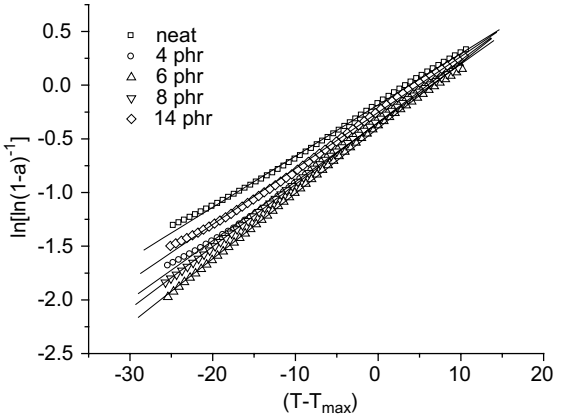

Fig. 5. Kinetics of thermal decomposition of epoxy nanocomposites by using Horowitz–Metzger method.

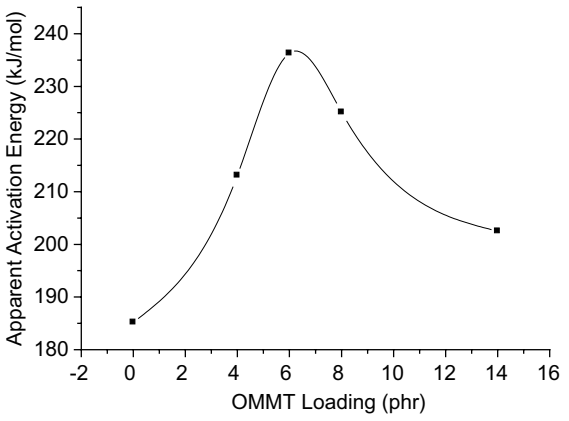

Fig. 6. Effects of OMMT loading on activation energy calculated circulated by using Horowitz–Metzger method.

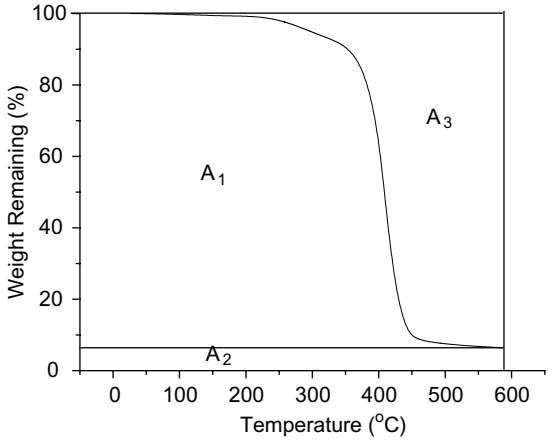

Fig. 7. The schematic diagram of the Doyle's method for determining the IPDT.

where, T_i and T_f are the initial experimental temperature and the final experimental temperature respectively. The relationship between IPDT and the OMMT loading is shown in Fig. 8. The IPDT clearly increases with OMMT loading.

3.3. Correlation of thermal stability with OMMT dispersion

The above changes of the activation energy of the epoxy nanocomposites may be due to the structure evolution as the OMMT loading increases. When the OMMT loading is relatively low (below 8 phr), the nanocomposite develops an exfoliation dominant structure. The retardant effects of the exfoliated platelet to heat and oxygen in the epoxy matrix is strengthened when the OMMT loading increases since the number of

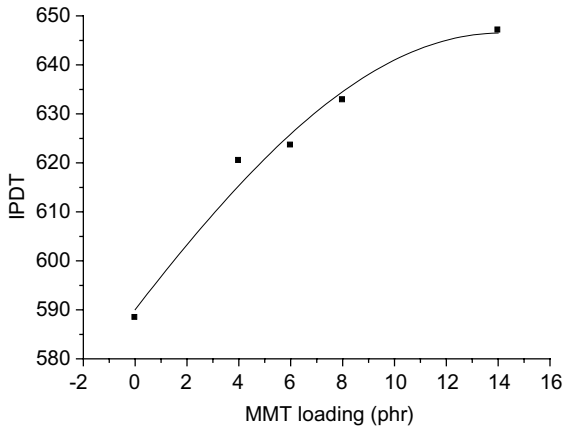

Fig. 8. Effects of OMMT loading on IPDT.

the exfoliated platelets increases with OMMT loading. When the OMMT loading increases further, the nanocomposites develop an exfoliated/intercalated structure. The number of exfoliated silicate platelet decreases with the OMMT loading. The tactoids, which is less effective in blocking heat and oxygen than the exfoliated platelet, however, increases with the OMMT loading. As a consequence, the activation energy decreases when the OMMT loading is higher than 8 phr. As the tactoids still show the retardant effects to heat and oxygen, the activation energy of the sample with exfoliated/intercalated structure is still higher than that of the neat epoxy resin.

This trend of IPDT is something different from the evolution of the activation energy. This may be due to the difference of the physic natures of activation energy and IPDT. The activation energy describes the fast decomposition process of the resin network, ignoring the initial decomposition and the char yield formation. IPDT, however, reflects the whole stability of the sample, including the initial, fast decomposition and final (char forming) steps. As the OMMT in the epoxy matrix mainly contributes the retardant effects to heat and oxygen and char forming, the IPDT increases with OMMT loading. The activation energy, however, reaches a maximum at 6 phr OMMT because the dispersion state of the OMMT is the main concern in determining the fast decomposition process of the epoxy resin.

4. Conclusion

In the epoxy nanocomposites derived from the montmorillonite modified with the acidified cocamidopropyl betaine (CAB), the dispersion of the OMMT is dependent on the OMMT loading. The OMMT is evenly dispersed in the matrix with OMMT content lower than 8 phr (relative to 100 phr resin). When the

OMMT loading is higher than 8 phr, however, apparent aggregation of OMMT is observed. The thermal stability of the epoxy nanocomposite is dependent upon the dispersion state of the OMMT in the epoxy matrix although all the epoxy nanocomposites had enhanced thermal stability compared with the neat epoxy resin. The integral procedural decomposition temperature (IPDT), characterizing the whole stability of the nanocomposites, increases with OMMT loading. However, the activation energy, characterizing the stability of the fast decomposition stage of the nanocomposites, reaches a maximum at 6 phr OMMT. The evolution of the activation energy may be correlated with the change of the number of silicate platelet in the system.

References

[1] Pinnavaia TJ. Science 1983;220:365.
[2] LeBaron PC, Wang Z, Pinnavaia TJ. Appl Clay Sci 1999;15:11.
[3] LeBaron PC, Pinnavaia TJ. Chem Mater 2001;13:3760.
[4] Kawasumi M, Hasegawa N, Kato M, Usuki A, Okada A. Macromolecules 1997;30:6333.
[5] Tyan HL, Liu YC, Wei KH. Chem Mater 1999;11:1942.
[6] Zeng CC, Lee LJ. Macromolecules 2001;34:4098.
[7] Guo BC, Ouyang X, Cai CG, Jia DM. J Polym Sci Part B: Polym Phys 2004;42(7):1192.
[8] Coats AW, Redfern JP. Nature 1964;201(4914):68.
[9] Horowitz HH, Metzger G. Anal Chem 1963;35:1464.
[10] Dolye CD. Anal Chem 1961;33:77.